Photochemistry and Photobiology, 2005, 81: 384–393

Interaction of UV Radiation and Inorganic Carbon Supply in the Inhibition of Photosynthesis: Spectral and Temporal Responses of Two Marine Picoplankters¶

Cristina Sobrino*[1,2], Patrick J. Neale[2] and Luis M. Lubián[1]

[1]Instituto de Ciencias Marinas de Andalucía (CSIC), Puerto Real, Cádiz, Spain and
[2]Smithsonian Environmental Research Center, Edgewater, MD

Received 25 August 2004; accepted 1 November 2004

ABSTRACT

The effect of ultraviolet radiation (UVR) on inhibition of photosynthesis was studied in two species of marine picoplankton with different carbon concentration mechanisms: *Nannochloropsis gaditana* Lubián possesses a bicarbonate uptake system and *Nannochloris atomus* Butcher a CO_2 active transport system. Biological weighting functions (BWFs) for inhibition of photosynthesis by UVR and photosynthesis *vs* irradiance (PI) curves for photosynthetically active radiation (PAR) were estimated for both species grown with an enriched CO_2 supply (high dissolved inorganic carbon [DIC]: 1% CO_2 in air) and in atmospheric CO_2 levels (low DIC: 0.03% CO_2). The response to UVR and PAR exposures was different in each species depending on the DIC treatment. Under PAR exposure, rates of maximum photosynthesis were similar between treatments in *N. gaditana*. However, the cultures growing in high DIC had lower sensitivity to UVR than the low DIC cultures. In contrast, *N. atomus* had higher rates of photosynthesis under PAR exposure with high DIC, but the BWFs were not significantly different between treatments. The results suggest that one or more processes in *N. gaditana* associated with HCO_3^- transport are target(s) for UV photodamage because there was relatively less UV inhibition of the high DIC-grown cultures in which inorganic carbon fixation is supplied by passive CO_2 diffusion. Time courses of photochemical efficiency in PAR, during UV exposure and during subsequent recovery in PAR, were determined using a pulse amplitude modulated fluorometer. The results were consistent with the BWFs. In all time courses, a steady state was obtained after an initial decrease, consistent with a dynamic balance between damage and repair as found for other phytoplankton. However, the relationship of response to exposure showed a steep decline in activity that is consistent with a constant rate of repair. A novel feature of a model developed from a constant repair rate is an explicit threshold for photosynthetic response to UV.

INTRODUCTION

At present, stratospheric ozone depletion and the relative rapid increase in atmospheric CO_2 levels are two of the most important human impacts on our environment. Ozone depletion is dramatically shown in springtime polar ''holes'', although there has also been a steady decline at midlatitudes (1). This decrease in ozone concentration leads to the increase of short-wavelength solar ultraviolet radiation (UVR) that reaches the earth's surface (2). At the same time, the rise in CO_2 is faster than during any other period in Earth's history. A primary concern is that increased CO_2 will lead to increased surface temperature as result of the greenhouse effect; however, another consequence may be a delay in the recovery of stratospheric ozone despite the Montreal protocol ban on release of ozone-destroying chemicals (1).

Both factors are critical for aquatic ecosystems because photoautotrophic phytoplankton are the base of aquatic food webs and need sunlight and CO_2 for carbon assimilation into organic compounds. Solar UVR is known to affect several processes in aquatic organisms including photosynthesis, growth, motility, pigment composition and DNA damage. Though controversial, phytoplankton carbon acquisition may be affected by increased atmospheric CO_2 concentrations (3,4). Photosynthesis seems to be one of the principal targets of UV photodamage, with diverse effects on the different components of photosynthetic apparatus (reviewed by Vincent and Neale [5]).

In the past few years, several mathematical models have been developed to describe the inhibition of photosynthesis by UVR (6). In these models, a biological weighting function (BWF) translates spectral irradiance into biologically effective exposure (E^*_{inh} or H^*_{inh}). Photosynthesis is then modeled by including an exposure-dependent inhibition term in a photosynthesis *vs* irradiance (PI) function; the overall approach is termed the BWF–PI model. The use of either weighted irradiance (E^*_{inh}) or weighted cumulative exposure (H^*_{inh}) in the BWF–PI model depends on the interaction between the damage caused by the UV and the repair activated in the cells (7–9). The BWF_H model explains the photoinhibitory response in cells in which the repair is practically negligible. The

¶Posted on the website on 11 November 2004.
*To whom correspondence should be addressed: Smithsonian Environmental Research Center, 647 Contees Wharf Road P.O. Box 28, Edgewater, MD 21037-0028, USA. Fax: 443-482-2380; e-mail: sobrinoc@si.edu

Abbreviations: ATP, adenosine triphosphate; BWF, biological weighting function; CA, carbonic anhydrase; CCM, carbon concentration mechanism; DIC, dissolved inorganic carbon; ERC, exposure response curve; PAM, pulse amplitude modulated; PAR, photosynthetically active radiation; PCA, principal component analysis; PI, photosynthesis *vs* irradiance; PSII, photosystem II; UVR, ultraviolet radiation.

quantity of damaged targets is then time dependent and, consequently, photosynthetic rates decrease as a nonlinear function of the cumulative exposure (8,9). In contrast, in the BWF_E model repair is proportional to damage and the rate of photosynthesis decays in response to UV, reaching in about 30 min a steady state consistent with a dynamic balance between damage and repair (7,9,10).

The E and H models are based on simple kinetic assumptions that may not always apply. For example, some repair may be present, but it is insufficient to establish a steady state over the exposure period. In this case, it may be necessary to specify explicitly a repair rate (''R'' model) (11). This study describes another case in which repair is sufficient to attain a steady state but is regulated differently than in the E model. In this case repair is proportional to damage for low exposures, but at some threshold exposure, repair reaches a maximum rate and is constant at higher exposures. To account for this response, we developed a fourth type of BWF–PI model, called the BWF_T model, in which the response is approximated by assuming that repair rate is constant. The relevance of the exposure at which the repair saturates as well as the existence of thresholds is discussed.

Nannochloropsis gaditana (Eustigmatophyceae) and *Nannochloris atomus* (Chlorophyceae) are two marine picoplanktonic species with very similar morphology but different pigment composition and carbon concentration mechanisms (CCMs). *Nannochloropsis gaditana* is characterized by the lack of chlorophyll *b* and *c* (12,13) with the chlorophyll *a* and the violaxanthin the principle pigments being responsible for photosynthetic light absorption (14), whereas *N. atomus* shows the typical pigment pattern of the green algae with chlorophyll *a* and *b* (15,16). In addition, *N. gaditana* actively incorporates bicarbonate to be used as the main carbon source for photosynthesis (17), whereas *N. atomus* actively uptakes CO_2 (18).

There are few studies of UV inhibition of photosynthesis in marine picoplankton containing only chlorophyll *a*, and no studies have compared species with different CCM. Here, we analyze the synergistic effect of UVR and variation in CO_2 concentration on photosynthesis comparing results obtained for both species grown in low (0.03% CO_2 in air) and high (1% CO_2 in air) dissolved inorganic carbon (DIC) levels. This enabled comparisons of the response to UV in picoplankton with active (low DIC) and downregulated (high DIC) CCM (19). Comparisons are made on the basis of the spectral dependence of inhibition of photosynthesis determined by BWFs (6) and measurements of kinetics of photosynthetic response.

MATERIALS AND METHODS

Culture growth conditions. Cultures of *N. gaditana* Lubián (Eustigmatophyceae) and *N. atomus* Butcher (Chlorophyceae) were provided by the Marine Microalgae Culture Collection of the Instituto de Ciencias Marinas de Andalucía and grown with constant aeration in two different treatments: (1) high DIC (air with 1% CO_2) and (2) low DIC (air with 0.03%, *i.e.* atmospheric CO_2 levels). Cultures were grown at 20°C under continuous illumination with cool-white fluorescent lamps at an irradiance of 11 W m^{-2} of photosynthetically active radiation (PAR) (QSL 100, Biospherical Instruments, San Diego, CA). The growth medium was filtered seawater from the Gulf Stream with salinity adjusted to 35‰ and enriched with f/2 nutrients. The experiments were carried out during the fourth day after a standardized inoculation, in the middle of exponential growth phase. Cell densities were determined using a Neubauer hemocytometer.

Cellular absorption and chlorophyll concentration. Particulate absorbance of UV and PAR was analyzed by the quantitative filter technique as described by Neale *et al.* (8). Cells concentrated on glass fiber filters (Whatman GF/F) were scanned in a Cary 4 dual beam spectrophotometer, using a blank filter wetted with filtrate as a reference.

Chlorophyll concentration was measured on aliquots concentrated on glass fiber filters extracted with methanol and maintained in dark at least overnight at 4°C. After centrifugation, absorption of the supernatant was measured at the appropriate wavelengths according to the equations of Talling and Driver (20) for *N. gaditana* and Holden (21) for *N. atomus*.

Photosynthetic response to UV. Photosynthetic response to PAR and inhibition by UVR was measured as the uptake of $H^{14}CO_3^-$ (approximately 0.5 μCi mL^{-1}) into organic compounds during the 1 h incubation period in a special spectral incubator, the photoinhibitron (6,22,23). The incubator uses a 2500 W xenon lamp (solar simulator lamp). A mirror directs the lamp beam upward to the bottom of a temperature-controlled aluminum block. The beam passes through an array of seven Schott WG series long-pass filters (280, 295, 305, 320, 335, 350 and 370) and one GG series (395) that are combined with neutral density screens to produce nine irradiances for a total of 72 treatments of varying spectral composition and irradiance. The treatments are directed to 1 cm diameter, flat-bottom quartz cuvettes that are mounted within the block and filled with 1 mL of culture for exposure. Spectral irradiance was measured (1 nm resolution) with a specially configured quartz fiber-optic coupled to a scanning monochromator (SPG 300, Acton Research, Acton, MA) with a photomultiplier tube detector. The system is calibrated with a mercury standard lamp for wavelength and 1000 W halogen lamp (traceable to the National Institute of Standards and Technology) for absolute irradiance. Data were collected by the Spectrasense program.

Simultaneously with the photoinhibitron incubations, more detailed PI curves for PAR-only exposure were obtained in separate ''photosynthetron'' incubations using a modification of the protocol described by Lewis and Smith (24). One milliliter culture samples were incubated in 7 mL scintillation vials exposed to 37 different irradiances that were obtained by filtering irradiance from a 250 W halogen lamp with neutral density screens. Irradiance was measured with a quantum scalar sensor (QSL-100) mounted inside a scintillation vial.

All incubations were carried out at 20°C and were terminated by adding 0.25 mL of 1.2 *N* HCl to each cuvette. The vials were shaken overnight after which 5 mL of Ecolume scintillation cocktail was added. Incorporated ^{14}C was measured on a Tri-Carb 1600 TR liquid scintillation analyzer (Perkin Elmer, Boston, MA). Total DIC was determined with a Shimadzu (Columbia, MD) ASI-5000 analyzer.

Photosynthetic response to PAR. PI curves were determined from photosynthetron incubations. Photosynthetic parameters in PAR, P_s^B and E_s, were estimated using nonlinear regression. Data were fitted using the equation:

$$P^B = P_s^B \tanh\left(\frac{E_{PAR}}{E_s}\right) \quad (1)$$

where P^B is photosynthesis normalized to chlorophyll *a* content (gC $gChl^{-1}$ h^{-1}), P_s^B is the maximal rate of photosynthesis, E_s is the saturation irradiance for PAR and E_{PAR} is the PAR irradiance (W m^{-2}).

BWF_T–PI model. BWFs were estimated from the measured rates of photosynthesis using statistical methods similar to those described previously (6,22). The model is based on the PAR-only (no inhibition) PI curve (Eq. 1), adding a term that represents inhibition of photosynthesis by UV and PAR exposure:

$$P^B = P_s^B \tanh\left(\frac{E_{PAR}}{E_s}\right) \min\left(1, \frac{1}{E_{inh}^*}\right) \quad (2)$$

where min denotes the minimum function and E_{inh}^* is a dimensionless index that is defined as

$$E_{inh}^* = \sum_{\lambda=280}^{400} (\varepsilon(\lambda)E(\lambda)\Delta\lambda) + \varepsilon_{PAR}E_{PAR} \quad (3)$$

and is known as biologically effective or weighted irradiance. $\varepsilon(\lambda)$ is the biological weight (reciprocal mW m^{-2}) at wavelength λ, $E(\lambda)$ is the spectral irradiance at λ (mW m^{-2} nm^{-1}) and $\Delta\lambda$ is the wavelength resolution, 1 nm (6). Inhibition by PAR is included using a single broadband weight, ε_{PAR} (reciprocal W m^{-2}), for total PAR irradiance.

The inhibition term relates the effect of UV to weighted exposure (exposure response curve [ERC]) and accounts for the kinetics of UV

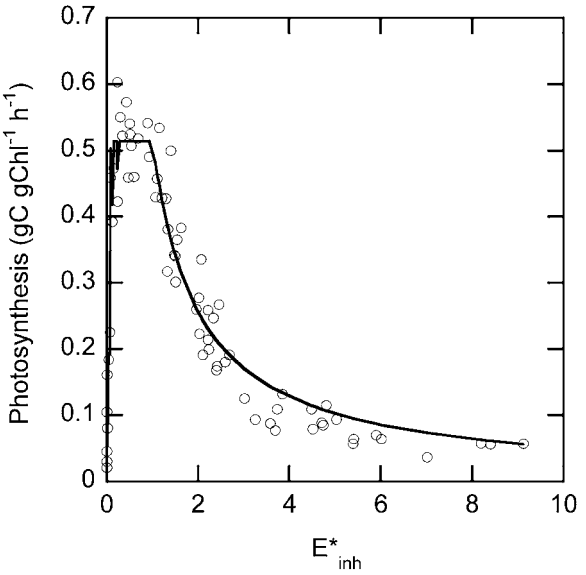

Figure 1. Exposure response curve (ERC) of a *Nannochloropsis gaditana* high DIC culture. Open circles are observed photosynthetic rates (gC gChl^{-1} h^{-1}) obtained during 1 h incubation in the photoinhibitron, and the continuous line shows the predicted rate using the fitted BWF_T–PI model. Note that the threshold in the fitted model at weighted irradiance (E^*_{inh}) of 1 (dimensionless), inhibition of photosynthesis occurs only when $E^*_{inh} > 1$.

damage and repair during exposure. The ERC used in Eq. 2 differs with previously reported ERCs (9) in that it assumes a constant rate of repair (used in a general sense to include all processes that counteract the inhibitory effect of UV: resynthesis, reactivation, etc.) irrespective of the amount of damage. Neale (9) derived this ERC based on a steady state between damage and a constant rate of repair. This derivation is extended in the discussion of the results presented in this article. One consequence of these assumptions is that repair completely compensates for damage (ERC is unity) until E^*_{inh} reaches a threshold level of 1, above which photosynthesis declines (Fig. 1). The model is designated the BWF_T–PI model, with the ''T'' symbolizing the presence of the threshold.

Spectral irradiance curves were analyzed using principal component analysis (PCA) and the derived spectral scores used to fit the BWF_T–PI model. Error estimates of the BWFs were derived by propagation of errors as described previously (6,22,25).

Photosynthetic efficiency of photosystem II. To obtain kinetic data to support the model, time courses of photosynthesis during UV exposure were measured. Our approach used fluorescence yield as measured using the pulse amplitude modulated (PAM) fluorometer (PAM 101, Walz, Effeltrich, Germany). Approximately 1.2 mL of culture was placed in a 1 cm square quartz cuvette, mounted in a temperature regulated holder and illuminated from below using irradiance from a 150 W xenon lamp (Schoeffel) filtered through selected filters and reflected by a mirror. The data are expressed as the relative efficiency of excitation energy capture by photosystem II (Φ_{PSII}) calculated as $(F'_m - F_s)/F'_m$ which has been correlated with variations in the quantum yield of photosynthesis (26). F_s is the steady-state *in vivo* chlorophyll fluorescence of phytoplankton during the illumination, and F'_m is the maximum yield of fluorescence obtained after a saturating light pulse (400 ms pulse duration) was applied every 30 s. All experiments were carried out with replicate cultures in exponential growth phase (n = 3–5). For each sample there were two different light treatments: (1) only PAR (control) and (2) PAR + UV. In each case, a dark-adapted sample was maintained without actinic illumination for 5 min to measure maximum $\Phi_{PSIImax}$ (= $[F_m - F_o]/F_m$) followed by periods (3–5 min) of increasing PAR irradiances (GG395 filter), avoiding PAR inhibition (27) and promoting acclimation. When the maximal irradiance of 104 W m^{-2} was reached, the GG395 filter was maintained during 45 min for the PAR control treatment, or the GG395 filter was replaced with two Schott WG320 filters resulting in the same level of PAR with added UVR (PAR + UV). After 45 min in UV the WG320 filters were replaced with the GG395 filter for the study of recovery with PAR for 30 min.

Table 1. Characteristics of *Nannochloris atomus* and *Nannochloropsis gaditana* cultures grown in high DIC (1% CO_2) and low DIC levels (0.03% CO_2) on the fourth day of growth. Values are the mean ± standard error of 4–7 independent experiments

	Cellular chlorophyll *a* (fg cell^{-1})	Cell density (cell mL^{-1})	External pH
Nannochloris atomus			
Low DIC	51.8 ± 4.1	18.3×10^6 ± 2.1	7.94 ± 0.03
High DIC	49.7 ± 4.7	26.4×10^6 ± 2.9	6.52 ± 0.04
Nannochloropsis gaditana			
Low DIC	87.0 ± 1.5	23.4×10^6 ± 2.3	8.61 ± 0.25
High DIC	83.5 ± 4.9	9.8×10^6 ± 1.2	6.61 ± 0.09

Time series of $H^{14}CO_3^-$ incorporation were also carried out in *N. gaditana* high DIC cultures using a similar irradiation protocol as for the PAM fluorescence measurements. A total of 3.3 mL of culture inoculated with 40 μCi of $H^{14}CO_3^-$ was dispensed into a 2.5 cm diameter cylindrical quartz cuvette and then exposed to PAR and PAR + UV as described before. Irradiance varied from 130 W m^{-2} in the center of the cuvette to 110 W m^{-2} in the sides, and the GG400 nm filter was used for the PAR exposure. No photoinhibition was observed in either the GG400 or GG395 filter treatment. Subsamples of 100 μL were taken every 10 min. Aliquots were dispensed into scintillation vials, previously poisoned with 5 μL borate-buffered formalin according to the protocol of Cullen and Lesser (10). These were later acidified with 1.25 mL 1.2 *N* HCl and shaken overnight in a hood. When all the inorganic ^{14}C was released, 5 mL of Ecolume scintillation cocktail was added.

Statistical analysis. The results obtained from the different DIC treatments were analyzed by a Student–Newman–Keuls test. BWFs were estimated for each experiment, and the mean BWF was calculated for each treatment (n = 2–3), with confidence limits for the mean derived from individual error estimates by propagation of errors (28).

RESULTS

Culture growth

Characteristics of *N. gaditana* and *N. atomus* cultures maintained in low (0.03% CO_2) and high (1% CO_2) DIC levels are shown in Table 1. Differences in chlorophyll content per cell were not significant in either species between CO_2 treatments. Cell density at harvest was significantly higher in high DIC (*vs* low DIC) cultures of *N. atomus* (Table 1, $P < 0.05$) and significantly lower in high DIC cultures of *N. gaditana* ($P < 0.001$). After 4 days of growth, all the cultures aerated with the CO_2 supply showed pH values close to 6.6. The pH was higher for *N. gaditana* than for *N. atomus* and higher in the low DIC cultures than in the high DIC cultures (Table 1).

Chlorophyll-specific light absorption

Chlorophyll-specific light absorption also changed with DIC concentration, but the pattern was the inverse of cell density. Cellular absorbance normalized to chlorophyll, shown in Fig. 2, was greater in *N. gaditana* cultures grown in high DIC than the low DIC culture. Absorbance in *N. atomus* cultures was more similar between treatments although smaller for the high DIC culture. The profile of spectral absorbance was similar between treatments for each species and did not reveal presence of any UV-absorbing compounds. Note that the absorbance spectra for *N. gaditana* cultures are consistent with the absence of the accessory chlorophylls *b* and *c*, whereas the shape of the *N. atomus* spectra

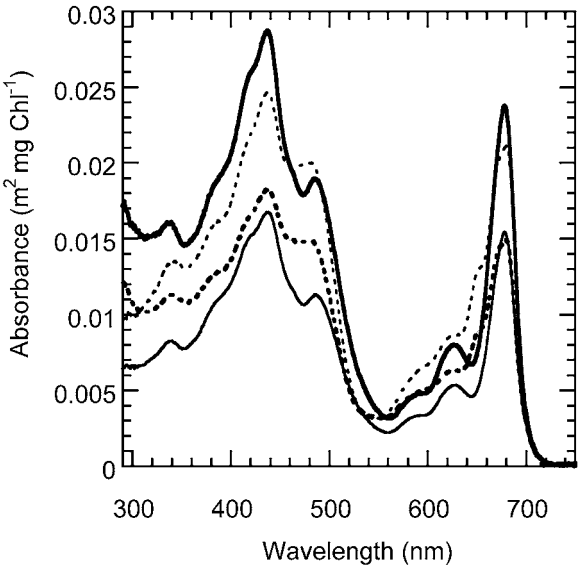

Figure 2. Average spectral absorbance (m^2 $mgChl^{-1}$) by *Nannochloropsis gaditana* and *Nannochloris atomus* cultures maintained with and without 1% CO_2 supply. The solid double line shows the spectral absorbance of *N. gaditana* high DIC (1% CO_2), and the solid single line corresponds to *N. gaditana* low DIC (0.03% CO_2). The dashed double line shows the spectral absorbance of *N. atomus* high DIC (1% CO_2), and the dashed normal line corresponds to *N. atomus* low DIC (0.03% CO_2).

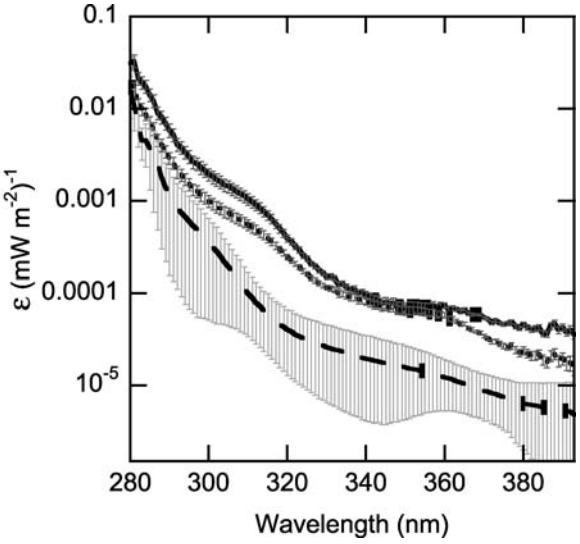

Figure 3. Biological weighting functions for the inhibition of photosynthesis by UV ($\varepsilon(\lambda)$, reciprocal mW m^{-2}) estimated by statistical analysis of data from different phytoplanktonic species. The solid line is the average biological weight for *Nannochloropsis gaditana* (n = 2), the short dashed line is the average biological weight for *Nannochloris atomus* (n = 3) and the long dashed line is the mean of the average BWFs from different cultures of marine dinoflagellates and diatoms (43). Values are the mean BWF (±standard deviation) for the dinoflagellates and diatoms, whereas *N. gaditana* and *N. atomus* values correspond to the mean BWF of control cultures with a 95% confidence interval.

(*e.g.* peak at 676 nm, shoulder at 650 nm) indicated the presence of both chlorophyll *a* and chlorophyll *b*.

Photosynthetic response to PAR and UVR

Photosynthetic parameters in PAR estimated by fitting Eq. 1 to results from the photosynthetron incubations are shown in Table 2. Photosynthetic parameters of *N. gaditana* were not significantly different between cultures growing in different CO_2 concentrations. In *N. atomus*, P_s^B increased from 0.95 gC $gChl^{-1}$ h^{-1} for the low DIC to 1.58 gC $gChl^{-1}$ h^{-1} for high DIC. A similar relative increase occurred in E_s, indicating that the initial slope of the PI curve ($= P_s^B/E_s$) was about the same in each treatment. For all the treatments, cells exposed to PAR irradiances up to 200 W m^{-2} did not show any photoinhibition.

BWFs for inhibition of photosynthesis were obtained by fitting the photoinhibitron results to the BWF_T–PI model (Eq. 2). For each case, BWFs fitted with two to three spectral (PCA) components were sufficient to explain 91–95% of the variance of photosynthesis (e.g. Fig. 1). Comparisons with previously published BWFs for inhibition of photosynthesis indicated that *N. gaditana* and *N. atomus* were very sensitive to UVR (Fig. 3). BWF show that sensitivity is much smaller, on average, for the dinoflagellates and diatoms than for the picoplanktonic species, and among the later, *N. gaditana* is the more UV sensitive. Differences in $\varepsilon(\lambda)$ between the netplankton and the picoplanktonic cultures are smaller in the short-wavelength UV-B that is more harmful.

Photosynthetic rates relative to P_s^B(P^B/P_s^B) over 1 h UV + PAR exposure in the photoinhibitron for *N. gaditana* cultures grown in high and low DIC levels are shown in Fig. 4. The results for exposures to UV transmitted by the 370 and 335 nm long-pass filters were chosen as being representative of the spectral differences in response for both DIC treatments. Rates decreased with exposure to shorter wavelengths and higher irradiance and more in the low DIC than in the high DIC treatment (Fig. 4). Hence, relative photosynthetic rates at high irradiance (*e.g.* 300 W m^{-2} PAR) in the 370 and 335 nm long-pass filter treatments were approximately two times higher for the high DIC culture than the low DIC (Fig. 4). Consequently, the BWFs for *N. gaditana* differed between DIC treatments (Fig. 5). Although the BWFs had a similar shape, the culture growing in high DIC was significantly less sensitive to UV than the culture growing in low DIC levels over the 320–380 nm range. In both treatments the sensitivity was similar and progressively decreased from 295 to 320 nm, with a continued decline in the high DIC culture between 320 and 340 nm. From 340 to 380 nm, both functions became flatter showing no dependence between UV sensitivity and wavelength. Differences in weights between the low and high DIC *N. gaditana* cultures were greatest in this ''flat'' UV-A region. The average weight for PAR inhibition (ε_{PAR}) in *N. gaditana* cultures was 1.3×10^{-3}

Table 2. Photosynthetic parameters (average ± standard error) estimated from photosynthetron measurements for *Nannochloris atomus* and *Nannochloropsis gaditana* high DIC and low DIC cultures. P_s^B (gC $gChl^{-1}$ h^{-1}) is the saturated rate of photosynthesis, and E_s (W m^{-2}) is the light saturation parameter. Estimates were obtained using the observed data from photosynthetron (n = 40 per curve) fitted to equation for PI model $P^B = P_s^B \tanh(E_{PAR}/E_s)$

	Nannochloris atomus		*Nannochloropsis gaditana*	
	Low DIC	High DIC	Low DIC	High DIC
P_s^B	0.95 ± 0.01	1.58 ± 0.01	2.97 ± 0.03	2.96 ± 0.05
E_s	13.29 ± 0.39	20.9 ± 0.45	52 ± 1.82	49.73 ± 1.86
R^2	0.97	0.99	0.99	0.99

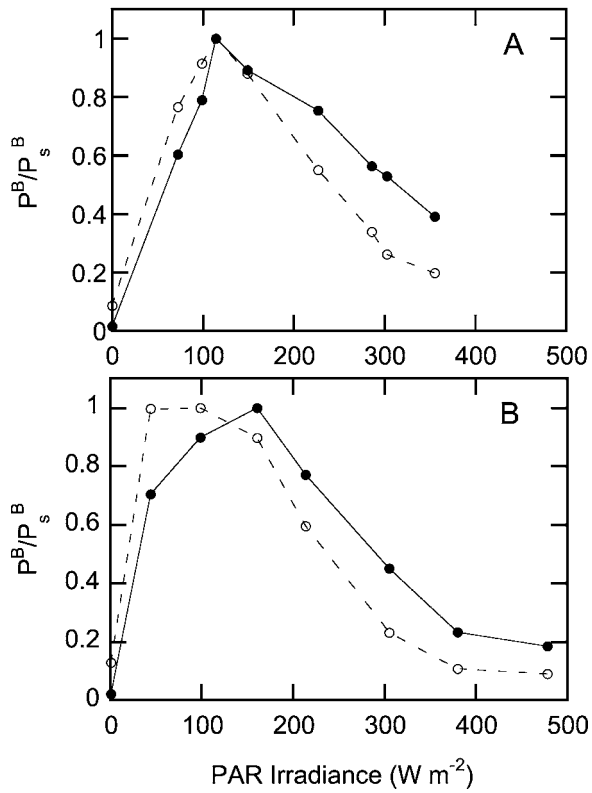

Figure 4. Relative photosynthetic rates P^B/P^B_s *vs* unweighted irradiance for *Nannochloropsis gaditana* cultures grown in high (1% CO_2) and low (0.03% CO_2) DIC concentration over 1 h of PAR + UV exposure in the photoinhibitron incubator. P^B_s is the maximal rate of photosynthesis in the absence of inhibition obtained by fitting the BWF_T–PI model. Photosynthetic rates from samples exposed to PAR + UV irradiance filtered by two different UV cutoff filters. A: Photosynthetic rates from samples exposed to irradiance filtered by a WG370 filter. B: Photosynthetic rates from samples exposed to irradiance filtered by a WG335 filter. The solid circles correspond to high DIC cultures (1% CO_2) and the open circles correspond to low DIC cultures (0.03% CO_2).

(reciprocal W m^{-2}) with a 95% confidence interval of $\pm 2.1 \times 10^{-3}$. For both treatments, this low sensitivity to PAR inhibition was not statistically different from zero. In accordance with the statistical result, light-saturated rates of photosynthesis measured for exposures with the GG395 filter decreased only when E_{PAR} exceeded 400 W m^{-2} and, in any case, by less than 10% of the maximum (results not shown).

In contrast, sensitivity to UV in *N. atomus* was not different between cultures grown with different DIC concentration (Fig. 6). Weights decreased at longer wavelengths without consistent differences between treatments over the spectrum. This was also the case for sensitivity for PAR inhibition. In general, *N. atomus* was more sensitive to PAR inhibition than *N. gaditana*, with an average weight (±95% confidence interval) of $3.8 \times 10^{-3} \pm 1.0 \times 10^{-3}$ (reciprocal W m^{-2}), which corresponds to a threshold for PAR inhibition of 266 W m^{-2}.

Photosynthetic response time course; estimation of the rates of damage and repair

Fluorimetric time course measurements were carried out in PAR-only (control) and PAR + UV exposures. The absolute values with standard errors are shown in Table 3. The maximum PSII quantum

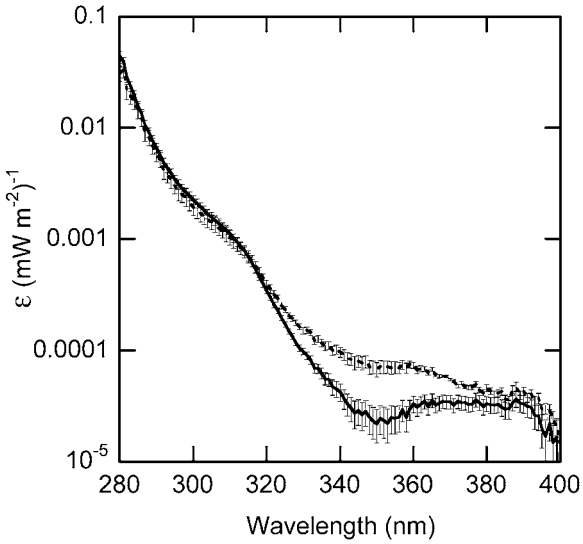

Figure 5. Average biological weight for the inhibition of photosynthesis by UV (ε(λ), reciprocal mW m^{-2}) estimated by statistical analysis of data from *Nannochloropsis gaditana* cultures maintained with and without 1% CO_2 supply in the medium. The solid line shows values obtained from high DIC cultures (1% CO_2) (n = 3), and the dashed line shows values from low DIC cultures (0.03% CO_2) (n = 2). The vertical bars show the 95% confidence interval for the average.

yield ($\Phi_{PSIImax}$) for darkened *N. gaditana* cultures was significantly ($P < 0.05$) higher in the low DIC cultures than in high DIC treatment. Larger differences were found for PSII efficiency (Φ_{PSII}) under PAR exposure, with *N. gaditana* low DIC cultures reaching values of 0.39 *vs* 0.20 with high DIC ($P < 0.01$). Despite this difference, rates of photosynthesis in PAR were the same in low and high DIC cultures (Table 2), apparently because higher PAR absorption compensated for the lower quantum yield (Fig. 2).

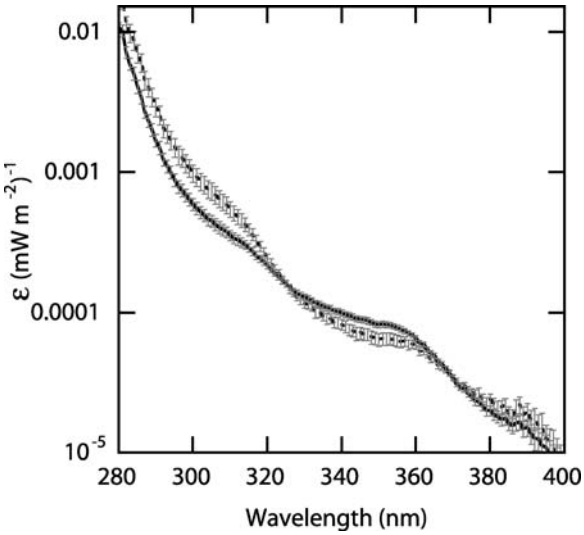

Figure 6. Average biological weight for the inhibition of photosynthesis by UV (ε(λ), reciprocal mW m^{-2}) estimated by statistical analysis of data from *Nannochloris atomus* cultures maintained with and without 1% CO_2 supply in the medium. The solid line shows values obtained from high DIC cultures (1% CO_2) (n = 2), and dashed line shows values from low DIC cultures (0.03% CO_2) (n = 3). The vertical bars show the 95% confidence interval for the average.

Table 3. Values (mean ± standard error) of the photosynthetic efficiency of PSII for *Nannochloris atomus* and *Nannochloropsis gaditana* growing in high DIC (1% CO_2) and low DIC levels (0.03% CO_2) during PAR and PAR + UV exposure ($F'_m - F_s/F'_m$) and maximal quantum yield ($F_m - F_0/F_m$) of dark-adapted cultures. PAR t_0 and UVR t_0 are values in the beginning of maximal PAR irradiance and PAR + UV exposure, respectively. PAR t_{45} and UVR t_{45} are the values after 45 min of PAR control or PAR + UV, and Recovery t_{30} are the values after 30 min of PAR, after UV exposure

	Nannochloris atomus		*Nannochloropsis gaditana*	
	Low DIC	High DIC	Low DIC	High DIC
Dark	0.67 ± 0.01	0.66 ± 0.01	0.63 ± 0.01	0.50 ± 0.05
PAR t_0	0.30 ± 0.03	0.33 ± 0.01	0.39 ± 0.02	0.21 ± 0.04
PAR t_{45}	0.25 ± 0.03	0.26 ± 0.03	0.39 ± 0.03	0.20 ± 0.04
UVR t_0	0.24 ± 0.04	0.30 ± 0.01	0.36 ± 0.02	0.18 ± 0.04
UVR t_{45}	0.18 ± 0.03	0.20 ± 0.02	0.21 ± 0.02	0.13 ± 0.03
Recovery t_{30}	0.23 ± 0.03	0.21 ± 0.02	0.33 ± 0.02	0.19 ± 0.03

Interesting changes were observed when UV was added to PAR. Although absolute yields were lower in the presence of 1% CO_2 (high DIC), the relative decrease in PSII quantum yields was greater in low DIC cultures (Fig. 7A). For *N. gaditana* low DIC cultures, quantum yields decreased 41.4% after 45 min of UV exposure, whereas the high DIC culture just showed a 27.3% decrease ($P < 0.001$). Relative values were obtained by dividing the effective quantum yields for each treatment, recorded every 30 s, by the initial UV yield. The initial UV yield was the first value of effective quantum yield of the same treatment measured when exposure began.

PSII quantum yields for *N. atomus* were not significantly different between cultures in any of the light treatments studied (Table 3). However, unlike *N. gaditana*, PSII yields decreased during both the PAR control and PAR + UV exposures. The PAR-only decrease was particularly evident for the *N. atomus* high DIC cultures in which absolute yields only attained an 11% recovery in the PAR + UV exposure after return to PAR exposure (Table 3). A comparison of time courses of PSII quantum yield for PAR control and PAR + UV exposure of *N. atomus* high DIC cultures is shown in Fig. 7B. The decrease in PSII quantum yield during PAR control exposure can be explained by a depletion of dissolved CO_2 during the exposure period (*i.e.* in an open-top cuvette, no aeration), which eventually caused a reduction in photosynthetic rate. The effect was most pronounced for the algae acclimated to high DIC during growth because CCM activity was downregulated by high external DIC concentration (19). To estimate the relative change in PSII quantum yield due to UV inhibition and recovery in *N. atomus*, the time course in PAR + UV was normalized to the yield after an equivalent period of PAR control exposure. Extrapolation of the PAR control time course was necessary as illustrated in Fig. 7B. After such adjustment, the variation in relative quantum yields during UV exposure was similar for low and high DIC cultures of *N. atomus*, especially considering the approximate nature of the normalization (Fig. 7C).

For each sample, at least 30 min was necessary to reach a steady-state PSII quantum yield under UV exposure (Fig. 7). After the PAR + UV treatment, exposure to 30 min of PAR allowed recovery of yield in all the cultures to almost the initial levels. Figure 7A,C show the increase of the photosynthetic rates reaching values close to 100% recovery or exceeding initial yield (110%) for *N. gaditana* high DIC.

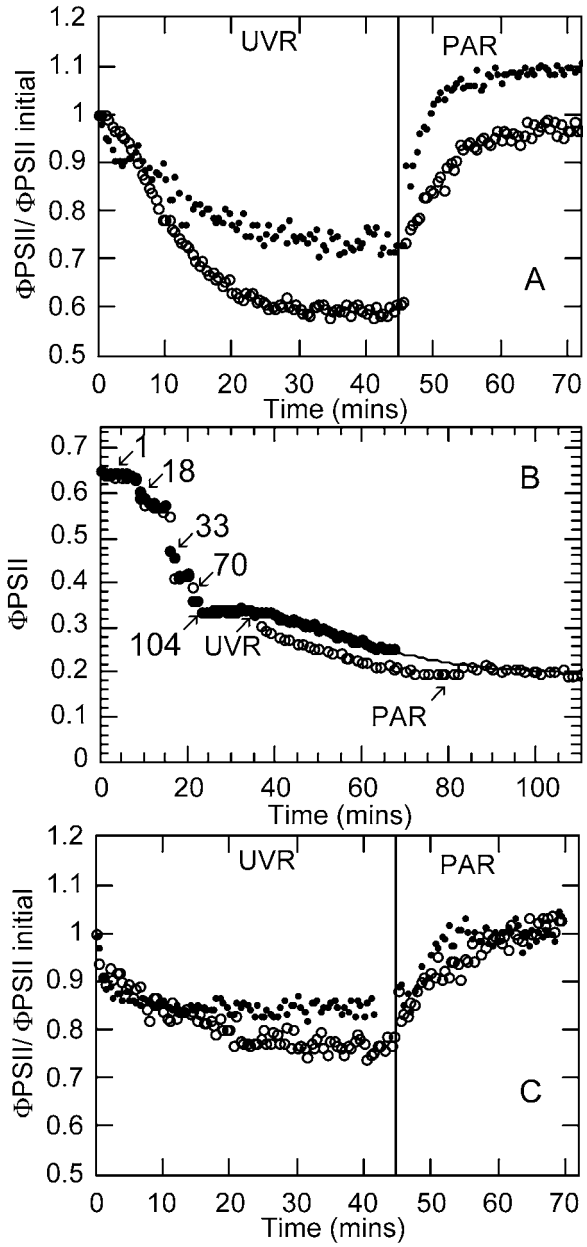

Figure 7. (A) Time course of relative PSII quantum yield (Φ_{PSII}) during 45 min of PAR + UV exposure (xenon lamp and WG320 long-pass filter), and subsequent recovery under 30 min PAR-only exposure (xenon lamp and GG395 nm long-pass filter), of *Nannochloropsis gaditana* grown with and without 1% CO_2 supply. Solid circles show the yields for high DIC (1% CO_2) and open circles show the yields for low DIC (0.03% CO_2). (B) Time course of PSII quantum yield for *Nannochloris atomus* high DIC cultures for PAR control exposure (solid circles) and during 35 min of PAR followed by 45 min of PAR + UV exposure and subsequent recovery under 30 min of PAR exposure (open circles). PAR was progressively increased over the first 35 min. Arrows indicate times of stepwise increases to the noted value of PAR irradiance (W m^{-2}). Continuous line trend during the PAR control exposure fitted by nonlinear regression and extrapolated over the full PAR + UV and PAR recovery exposure periods. (C) Time course of relative PSII quantum yield for *N. atomus* cultures after normalization of PSII quantum yield during PAR + UV exposure to the yield under a corresponding period of PAR control exposure (see text for further details). Solid circles show values for *N. atomus* high DIC (1% CO_2) and open circles correspond to *N. atomus* low DIC (0.03% CO_2).

The decrease in the fluorescence yields and subsequent increase during recovery were fitted to first-order functions of exposure time. The functions were of the form $P = a + b \exp(-r_{inh}t)$ for the UV exposure period and $P = a + b[1 - \exp(-r_{rec}t)]$ for the recovery, where P is PSII quantum yield and t is time (29,30). The fitted coefficients are the initial value (a) and decrement/increment (b) in P and the rates of inhibition (r_{inh}, min^{-1}) and recovery (r_{rec}, min^{-1}). The r_{inh} rates were 0.086 min^{-1} and 0.068 min^{-1} ($R^2 > 0.9$) for *N. gaditana* low and high DIC, respectively, whereas r_{rec} was similar for both treatments with rates close to 0.048 min^{-1}. Estimation of rates was not attempted for the relative time courses obtained for *N. atomus* because the normalization was approximate. However, the normalized time courses for low and high DIC cultures have qualitatively similar kinetics (Fig. 7C).

The time course of PAM measured PSII quantum yield was compared with the time course of $H^{14}CO_3^-$ uptake rates during 60 min of UV exposure. Although the UV + PAR irradiance was slightly higher in the ^{14}C uptake experiment, the relative variation in these two measurements showed qualitatively similar time course for a *N. gaditana* culture grown in high DIC (Fig. 8). After an initial increase, relative photosynthesis decreased reaching a steady state approximately 30 min after UV exposure began. Photosynthetic rates, however, increased during the last 20 min of UV exposure and with PAR recovery, again until rates exceeded initial values.

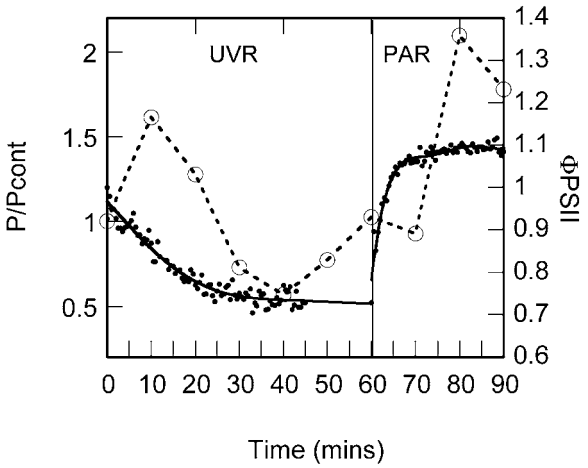

Figure 8. Time course of relative PSII quantum yield (Φ_{PSII}) monitored by PAM fluorometry (solid circles) and measured $H^{14}CO_3^-$ incorporation rates (open circles) for *Nannochloropsis gaditana* high DIC cultures during PAR + UV exposure (xenon lamp and WG320 long-pass filter) and subsequent recovery under PAR alone (xenon lamp and GG395 long-pass filter).

DISCUSSION

UV photodamage produced large decreases in carbon fixation in both species studied. The sensitivity of each alga to UVR is determined by many factors, first their own intrinsic capacity for defense and repair, used in the sense of all the processes that counteract UV damage, and second how defense and repair are influenced by environmental factors, which can increase damage, decrease efficiency of repair and indirectly promote repair and protection mechanisms (30,31). The BWFs presented show how all these factors act together over a 1 h period, in a wavelength-dependent manner, to affect carbon fixation. In parallel, the time course of PSII quantum efficiency (used as a proxy for photosynthesis) shows the kinetics of these interacting factors, as the resultant between damage and repair, during the UV exposure. In this article we present evidence that increased environmental CO_2 concentration can also increase the resistance to UVR in marine phytoplankton. This increase in UVR resistance is demonstrated as a decrease in the sensitivity of the BWF for inhibition of photosynthesis and as a reduced diminution of the chlorophyll fluorescence quantum yields in *N. gaditana* cultures. Under PAR conditions, *N. gaditana* and *N. atomus* photosynthetic rates are dependent on the availability of the preferred form of inorganic carbon for each algae. However, sensitivity to UVR was dependent on DIC concentration in *N. gaditana* and independent of DIC concentration in *N. atomus*.

Under PAR conditions the results show that growth and maximum quantum yield of PSII were negatively affected in *N. gaditana* cultures with 1% CO_2 supply (high DIC cultures). Similar, and even more dramatic, decreases in growth and PSII quantum yield have been described for cultures of *Chlorococcum littorale* transferred from air-grown conditions to extremely high CO_2 conditions (40% CO_2) (32,33). *Chlorococcum littorale* can acclimate to growth at high CO_2, but there is a lag period of about 4 days during which decreased growth and photosynthesis is associated with a decrease of PSII activity and an enhancement of PSI activity. Before acclimation, high activity of internal carbonic anhydrase (CA) results in acidification of the stroma under conditions of high CO_2 availability (34). This decreases the activity of RUBISCO, which increases excitation pressure on, and nonphotochemical quenching of, PSII. After acclimation, the PSI–PSII ratio increases to support an increase in adenosine triphosphate (ATP) synthesis by cyclic electron transfer as required for regulation of intracellular pH (33,35). Similar mechanisms may have caused a period of lower growth performance of *N. gaditana* cultures over the 4 days of growth in high DIC (see Materials and Methods), although carbon fixation rates measured after 4 days were similar in cultures grown in low and high DIC. The similar rate of photosynthesis in cultures grown at low and high DIC suggests that *N. gaditana* had acclimated to growth at low pH by the time the UV exposures were performed. At this point, intracellular pH may have increased due to a higher rate of ATP synthesis (through cyclic electron transfer and respiration). High internal CA activity occurs in air-grown *N. gaditana* because this alga relies on bicarbonate uptake as a source of CO_2 (17). Furthermore, the results show that increasing the CO_2 concentration of the medium does not enhance the carbon fixation rates in *N. gaditana* cells, which is in agreement with the lack of a system for active uptake of dissolved CO_2 in this algae. Conversely, the proportional increase in photosynthetic and growth rates with the CO_2 concentration in *N. atomus* supports that dissolved CO_2 is the form of inorganic carbon that is assimilated into organic compounds in this species (18).

Photosynthetic response to UV in these cultures was modeled with the BWF_T–PI model that assumes a constant rate of repair. This contrasts with previous presentations of irradiance-dependent BWFs (BWF_E–PI model, see Neale [9]), in which the ERC assumes that repair is proportional to damage. A more general perspective that couples the E and T models, considers two exposure ranges for photosynthetic response to UV. Initially, repair is proportional to damage, but at some threshold exposure, repair reaches a maximum rate and is constant for any higher exposure. Extending the kinetic analysis of Neale (9), with P_0-initial

photosynthesis, r-specific rate of repair, k-rate of damage and k_{max} rate of damage at which repair saturates at an absolute rate of r_{max}, we define a general rate of change of photosynthesis as:

$$\begin{aligned} k \le k_{MAX} \quad & \partial P/\partial t = -kP + r(P_0 - P) \\ k > k_{MAX} \quad & \partial P/\partial t = -kP + r_{max} \end{aligned} \tag{4}$$

and the time course of activity as:

$$\begin{aligned} \text{for } k \le k_{MAX} \quad & P(t)/P_0 = \frac{r}{k+r} + \frac{k}{k+r} e^{-(k+r)t} \\ \text{and for } k > k_{MAX} \quad & P(t)/P_0 = \frac{r_{max}}{k} + \frac{k - r_{max}}{k} e^{-kt} \end{aligned} \tag{5}$$

It follows from these equations that the steady-state response ($\partial P/\partial t = 0$) predicted by the BWF model should follow a general hyperbola ($1/[1 + E^*_{inh}]$) when $k \le k_{MAX}$ and a rectangular hyperbola ($1/E^*_{inh}$) when $k > k_{MAX}$. A biological justification of such an approach for photosynthesis is that many mechanisms of defense and repair are light regulated (*e.g.* xanthophylls de-epoxidation [36, Sobrino and coworkers, *Physiol. Plant.*, in press] and D1 turnover [37]) and increase with PAR and UV exposure. However, these processes cannot increase without limit and eventually a maximum (related to acclimation status) will be reached. The preceding analysis provides a basis for a general ERC; however, in many cases just one of the ERCs (BWF_E or BWF_T) may be sufficient to account for response over the relevant range of exposures. The most appropriate model can be determined by which one gives the higher R^2 and least bias in residuals. In case of the picoplankton species used for this study, sensitivity to UV exposure was high and repair apparently saturated at low exposure, so the BWF_T model was sufficient to produce a good fit in all treatments. Compared with the BWF_T model (*cf.* Fig. 1), fits of the BWF_E model using the experimental data from the picoplankton cultures showed significantly lower R^2 and a marked systematic bias with underestimation at moderate exposures and overestimation at high exposures (results not shown).

The BWF_T–PI model also predicts the presence of an explicit threshold below which no net effects are observed. The high variability of measured photosynthesis for exposures below the threshold impedes direct inference that rates are constant or otherwise (*cf.* Fig. 1, $E^*_{inh} < 1$). Indeed, it may be that a gradual decline with exposure did occur in this range as described in the previous paragraph. However, a fit of a general ERC was not attempted because application of this more complex approach was unlikely to significantly improve on the fits of the BWF_T model. More study is needed to determine whether thresholds actually exist for these species and whether rates are constant below the exposure threshold. Thresholds are ecologically significant because they define the conditions for spatial–temporal refuges from UV effects. The presence of thresholds for phytoplankton response to UV has been already suggested (38, 39). In *Phormidium murayi*, growth decreased after exceeding a threshold close to a UV-B–UV-A ratio of 0.18 (40). Furthermore, in Antarctic phytoplankton samples for UVR lower than 5–10 W m^{-2} (unweighted), photoinhibition was not observed (38).

The BWFs show that although both species studied have a similar and high sensitivity to UV compared with other phytoplankton, *N. gaditana* growing in high DIC is less sensitive to UVR than the low DIC culture, whereas *N. atomus* sensitivity seems to be unaffected by DIC concentration. This contention was also supported by the measurements of PSII quantum yield: during 45 min exposure to UV + PAR, the relative decrease in quantum yield is bigger in *N. gaditana* low DIC cultures than in cultures with the supplemental 1% CO_2 (high DIC). Moreover, the time course of relative PSII quantum yield shows the net result of the continuous interaction between UV damage and repair (8). In particular, the specific rates of inhibition (r_{inh}) and recovery (r_{rec}) of photosynthesis provide estimates of damage and repair rates, respectively, for each culture (*cf.* Eq. 5). These rates suggested that the greater decline in photosynthetic efficiency and higher BWF was due to a higher rate of damage in the low DIC than in the high DIC culture. The rate of repair was similar for the two cultures.

In *N. atomus*, on the contrary, the progressive decrease in PSII quantum yield that occurred even in the PAR control exposures did not allow a confident estimation of damage and repair rates and comparisons of these between treatments. This decrease, not related to UV photoinhibition, is attributed to the depletion of dissolved CO_2 from the medium. Indeed, such depletion probably also occurred during the photoinhibitron and photosynthetron incubations of *N. atomus*. Based on the rates of decrease observed in the PAR control time courses (*e.g.* Fig. 7B), such depletion could have depressed measurements of photosynthesis over a 60 min incubation by as much as 24% in the high DIC cultures and by a smaller amount in the low DIC cultures. The decrease should not affect the estimation of the BWF because these are based on relative responses to UV. The normalized time courses of *N. atomus* (Fig. 7C) show that a steady state was attained during UV exposure, and UV damage was reversed during subsequent PAR exposure. This indicates that responses to UV exposure were independent from the processes causing the overall decrease in PSII quantum yield as observed in the PAR control exposure. The fact that both species with similar morphology but different CCM show differences in UV sensitivity when they are grown at high and low DIC also implies that one or more of the processes involved with HCO_3^- transport in *N. gaditana* cells are a target for UV damage, whereas processes involved with active CO_2 transport in *N. atomus* are not. Hence, *N. gaditana* cultures maintained with the 1% CO_2 supply (high DIC cultures) showed less inhibition during UV exposure than low DIC cultures. This indicates that damage to processes related to HCO_3^- transport contributed to UV inhibition in low DIC cultures, whereas this type of damage had less of an effect on the high DIC cultures in which photosynthesis was supported by passive CO_2 flux across the membrane. Conversely, the CO_2 active transport system does not contribute to the UV sensitivity of photosynthesis in *N. atomus* because both cultures showed a similar response to UVR, whether or not the system was active. In addition, *N. gaditana* was more sensitive to UV than *N. atomus* under low DIC conditions, despite the similar size and growth conditions of the two cultures. This result is also consistent with greater UV effects when HCO_3^- transport is active, although the spectral regions of increased sensitivity are different for the comparison between species *vs* the comparison between low and high DIC (Fig. 3 *vs* Fig. 5). This suggests that there may be multiple sources for the differences in sensitivity between these species (5,40).

How the presence of HCO_3^- transport in *N. gaditana* increases sensitivity to UV is unknown. The inhibition could occur either because of damage to complexes directly involved in HCO_3^- transport or indirectly because of damage to cellular structures involved with transport, such as the cell wall and membrane (41). Moreover, the abundance of other UV-sensitive enzymes, such as RUBISCO, could change when HCO_3^- transport is active. In

addition, it is possible that high DIC cultures have a decreased sensitivity to UVR because they may have been already stressed by the low pH. This might decrease the differences between *N. gaditana* cultures when they are exposed to UVR.

Although there are few studies about the direct effects of UV on CCM, recently Beardall *et al.* (42) analyzed the effect of UV-B radiation on the CCM of *Dunaliella tertiolecta*. Under acute exposures to a UV-B source (with minimal UV-A and PAR exposure), there was a rapid decline in PSII activity. Such exposures had no direct effects on active transport of inorganic carbon as measured by uptake of $H^{14}CO_3^-$ during very short (10 s) incubations. Although there are significant differences in the exposure conditions between the Beardall *et al.* study (42) and this study, the response of *D. tertiolecta* is consistent with the present results in indicating that the CCM-related component of UV inhibition mainly contributes to sensitivity of photosynthesis to UV-A as opposed to UV-B (*cf.* Fig. 5).

In conclusion, this study presents evidence that external CO_2 supply can affect phytoplankton UV resistance, although responses vary between species. Increased CO_2 levels in the medium produced a decrease in the UV sensitivity, as shown by higher PSII quantum yields and carbon fixation rates. However, CO_2 enrichment counteracted UV inhibition only for *N. gaditana* cultures, in which UV appears to damage some undetermined component related to bicarbonate active transport. The implications of this conclusion for marine photosynthesis are presently uncertain because it is unknown whether UV effects are also lessened by small enhancements in the CO_2 supply characteristic of the current atmospheric increase and what fraction of phytoplankton will resemble *N. gaditana* in their response (as opposed to *N. atomus*). Nevertheless, the results show that there are multiple mechanisms involved in UV inhibition of photosynthesis that can be elucidated through manipulation of environmental factors together with UV exposure.

Acknowledgements—This research was supported by a grant to C.S. from the Spanish Ministry of Science and Technology (Project AMB97-1021-C02-02). P.J.N acknowledges support from the U.S. National Science Foundation, Biological Oceanography program (OCE-9812036). Linda Franklin is acknowledged for making helpful comments.

REFERENCES

1. Madronich, S., R. L. McKenzie, L. O. Björn and M. M. Caldwell (1998) Changes in ultraviolet radiation reaching the Earth's surface. Environmental effects of ozone depletion. *J. Photochem. Photobiol. B: Biol.* **46**, 5–19.
2. Diaz, S. B., J. H. Morrow and C. B. Booth (2000) UV physics and optics. In *The Effects of UV Radiation on Marine Ecosystems* (Edited by S. J. de Mora, S. Demers and M. Vernet), pp. 35–71. Cambridge University Press, Cambridge, UK.
3. Riebesell, U., D. Wolf-Gladrow and V. Smetacek (1993) Carbon dioxide limitation of phytoplankton growth rates. *Nature* **361**, 249–251.
4. Hein, M. and K. San Jensen (1997) CO_2 increases oceanic primary production. *Nature* **388**, 526–527.
5. Vincent, W. F. and P. J. Neale (2000) Mechanisms of UV damage to aquatic organisms. In *The Effects of UV Radiation on Marine Ecosystems* (Edited by S. J. de Mora, S. Demers and M. Vernet), pp. 149–176. Cambridge University Press, Cambridge, UK.
6. Cullen, J. J. and P. J. Neale (1997) Biological weighting functions for describing the effects of ultraviolet radiation on aquatic systems. In *Effects of Ozone Depletion on Aquatic Ecosystems* (Edited by D. P. Häder), pp. 97–118. R. G. Landes, Austin, TX.
7. Lesser, M. P., J. J. Cullen and P. J. Neale (1994) Carbon uptake in a marine diatom during acute exposure to UV-B radiation: relative importance of damage and repair. *J. Phycol.* **30**, 183–192.
8. Neale, P. J., A. T. Banaszak and C. R. Jarriel (1998) Ultraviolet sunscreens in *Gymnodinium sanguineum* (Dinophyceae): Mycosporine-like amino acids protect against inhibition of photosynthesis. *J. Phycol.* **34**, 928–938.
9. Neale, P. J. (2000) Spectral weighting functions for quantifying the effects of ultraviolet radiation in marine ecosystems. In *The Effects of UV Radiation on Marine Ecosystems* (Edited by S. J. de Mora, S. Demers and M. Vernet), pp. 73–100. Cambridge University Press, Cambridge, UK.
10. Cullen, J. J. and M. P. Lesser (1991) Inhibition of phytoplankton photosynthesis by ultraviolet radiation as a function of dose and dosage rate. *Mar. Biol.* **111**, 83–90.
11. Hiriart-Baer, V. P. and R. E. H. Smith (2004). Models for ultraviolet radiation-dependent photoinhibition of Lake Erie phytoplankton. *Limnol. Oceanogr.* **49**(1), 202–214.
12. Lubián, L. M. and R. Establier (1982). Comparative study of the pigment composition in several strains of *Nannochloropsis* (Eustigmatophyceae), during its growth in culture. *Inv. Pesq.* **46**(3), 379–389.
13. Lubián, L. M., O. Montero, I. Moreno-Garrido, I. E. Huertas, C. Sobrino, M. González-del-Valle and G. Parés (2000) *Nannochloropsis* (Eustigmatophyceae) as a source of commercially valuable pigments. *J. Appl. Phycol.* **12**, 249–255.
14. Owens, T. G., J. C. Gallagher and R. S. Alberte (1987). Photosynthetic light-harvesting function of violaxanthin in *Nannochloropsis sp.* (Eustigmathophyceae). *J. Phycol.* **23**, 79–85.
15. Jeffrey, S. W. (1961) Paper-chromatographic separation of chlorophylls and carotenoids from marine algae. *J. Biochem.* **80**, 336–342.
16. Establier, R. and L. M. Lubián (1982) Composición de pigmentos en *Nannochloris maculata* Butcher y *N. oculata* Droop (CCAP, 251/6). Implicaciones de tipo taxonómico. *Inv. Pesq.* **46**(3), 451–457.
17. Huertas, I. E., G. S. Espie, B. Colman and L. M. Lubián (2000). Light-dependent bicarbonate uptake and CO_2 efflux in the marine microalga *Nannochloropsis gaditana*. *Planta* **211**, 43–49.
18. Huertas, I. E., B. Colman, G. S. Espie and L. M. Lubián (2000). Active transport of CO_2 by three species of marine microalgae. *J. Phycol.* **36**, 314–320.
19. Beardall, J. and M. Giordano (2002) Ecological implications of microalgal and cyanobacteria CCMs and their regulations. *Funct. Plant Biol.* **29**, 335–347.
20. Talling, J. F. and D. Driver (1974) Some problems in the estimation of chlorophyll *a* in phytoplankton. In *Proceedings, Conference of Primary Productivity Measurement, Marine and Freshwater*, pp. 142–146. Hawaii.
21. Holden, M. (1976) Chlorophylls. In *Chemistry and Biochemistry of Plants Pigments*, Vol. II (Edited by T. W. Goodwin), pp. 1–37. Academic Press, London.
22. Cullen, J. J., P. J. Neale and M. P. Lesser (1992) Biological weighting function for the inhibition of phytoplankton photosynthesis by ultraviolet radiation. *Science* **258**, 646–650.
23. Neale, P. J. and J. J. Fritz (2001) Experimental exposure of plankton suspensions to polychromatic ultraviolet radiation for determination of spectral weighting functions. In *Ultraviolet Ground- and Space-based Measurements, Models, and Effects*, Vol. 4482 (Edited by J. Slusser, J. R. Herman and W. Gao), pp. 291–296. SPIE—The International Society for Optical Engineering, San Diego.
24. Lewis, M. R. and J. C. Smith (1983) A small volume, short incubation-time method for measurement of photosynthesis as a function of incident irradiance. *Mar. Ecol. Prog. Ser.* **13**, 99–102.
25. Neale, P. J., M. P. Lesser and J. J. Cullen (1994) Effects of ultraviolet radiation on the photosynthesis of phytoplankton in the vicinity of McMurdo Station (78°S). In *Ultraviolet Radiation in Antarctica: Measurements and Biological Effects* (Edited by C. S. Weiler and P. A. Penhale), pp. 125–142. American Geophysical Union, Washington, DC.
26. Genty, B., J. M. Briantais and M. R. Baker (1989). The relationship between the quantum yield of photosynthetic electron transport and quenching of chlorophyll fluorescence. *Biochim. Biophys. Acta* **990**, 87–92.
27. Neale, P. J. (1987) Algal photoinhibition and photosynthesis in the aquatic environment. In *Photoinhibition* (Edited by D. J. Kyle, C. B. Osmond and C. J. Arntzen), pp. 35–65. Elsevier, Amsterdam.
28. Bevington, P. R. (1969) *Data Reduction and Error Analysis for the Physical Sciences*. McGraw Hill, New York.

29. Heraud, P. and J. Beardall (2000) Changes in chlorophyll fluorescence during exposure of *Dunaliella tertiolecta* to UV radiation indicate a dynamic interaction between damage and repair processes. *Photosynth. Res.* **63**, 123–134.
30. Litchman, E., P. J. Neale and A. T. Banaszak (2002). Increased sensitivity to ultraviolet radiation in nitrogen-limited dinoflagellates: photoprotection and repair. *Limnol. Oceanogr.* **47**(1), 86–94.
31. Neale, P. J. (2001). Modeling the effects of ultraviolet radiation on estuarine phytoplankton production: impact of variations in exposure and sensitivity to inhibition. *J. Photochem. Photobiol. B: Biol.* **62**, 1–8.
32. Pesheva, I., M. Kodama, M. L. Dionisio-Sese and S. Miyachi (1994) Changes in photosynthetic characteristics induced by transferring air-grown cells of *Chlorococcum littorale* to high-CO_2 conditions. *Plant Cell Physiol.* **35**, 379–387.
33. Satoh, A., N. Kurano, H. Senger and S. Miyachi (2002). Regulation of energy balance in photosystems in response to changes in CO_2 concentration and light intensities during growth in extremely-high-CO_2-tolerant green microalgae. *Plant Cell Physiol.* **43**(4), 440–451.
34. Satoh, A., N. Kurano and S. Miyachi (2001) Inhibition of photosynthesis by intracellular carbonic anhydrase in microalgae under excess concentrations of CO_2. *Photosynth. Res.* **68**, 215–224.
35. Miyachi, S., I. Iwasaki and Y. Shiraiwa (2003). Historical perspective on microalgal and cyanobacterial acclimation to low- and extremely high-CO_2 conditions. *Photosynth. Res.* **77**, 139–153.
36. Niyogi, K. K. (1999) Photoprotection revisited: genetic and molecular approaches. *Annu. Rev. Plant Physiol. Plant Mol. Biol.* **50**, 333–359.
37. Greenberg, B. M., V. Gaba, O. Canaani, S. Malkin, A. K. Matto and M. Edelmann (1989) Separate photosensitizers mediate degradation of the 32kDa photosystem II reaction center protein in the visible and UV spectral regions. *Proc. Natl. Acad. Sci. USA* **86**, 3317–3320.
38. Hebling, E. W., V. Villafañe, M. Ferrario and O. Holm-Hansen (1992) Impact of natural UV-R on rates of photosynthesis and on specific marine phytoplankton species. *Mar. Ecol. Prog. Ser.* **80**, 89–100.
39. Quesada, A., J. Mouget and W. F. Vincent (1995) Growth of Antarctic cyanobacteria under ultraviolet radiation: UVA counteracts UVB inhibition. *J. Phycol.* **31**, 242–248.
40. Roy, S. (2000) Strategies for the minimization of UV-induced damage. In *The Effects of UV Radiation on Marine Ecosystems* (Edited by S. J. de Mora, S. Demers and M. Vernet), pp. 177–205. Cambridge University Press.
41. Sobrino, C., O. Montero and L. M. Lubián (2004) UV-B radiation increases cell permeability and damages nitrogen incorporation mechanisms in *Nannochloropsis gaditana*. *Aquat. Sci.* **66**, 421–429.
42. Beardall, J., P. Heraud, S. Roberts, K. Shelly and S. Stojkovic (2002) Effects of UV-B radiation on inorganic carbon acquisition by the marine microalga *Dunaliella tertiolecta* (Chlorophyceae). *Phycologia* **41**, 268–272.
43. Neale, P. J. and D. J. Kieber (2000) Assessing biological and chemical effects of UV in the marine environment: spectral weighting functions. In *Causes and Environmental Applications of Increased UV-B Radiation* (Edited by R. E. Hester and R. M. Harrison), pp. 61–83. The Royal Society of Chemistry, Cambridge, UK.